Bottled Brilliance: Gated Mixture of Experts for Biomedical Explainability

Sidharrth Nagappan
sn666@cam.ac.uk
University of Cambridge

Abstract

The source code is made available at https://github.com/sidharrth2002/biomedical-moe.

Keywords Biomedical Explainability · CLIP · BioMedCLIP · Mixture of Experts

1 Introduction

The adoption of deep learning in highly sensitive domains like computational medicine have led to increased calls for robust explainability mechanisms, that medical practitioners can use to trace the reasoning behind specific decisions [1]. While post-hoc interpretability methods are rampant in the literature, the detachment from the internal workings of the model can result in incomplete explanations [2], and the "completeness" paradigm is a crucial part of building trust in these automated systems. Concept Bottleneck Models (CBM) organically incentivise models to route decisions through an interpretable concept layer, where each neuron in the bottleneck corresponds to a human-understandable concept. However, annotating concepts can be costly, leading to Language in a Bottle (LaBO) introducing an end-to-end pipeline that leverages Large Language Models (LLMs) to build and enrich concept bottlenecks, before using Vision Language Models (VLMs) such as CLIP to align images and textual concepts [3]. Although effective against a range of datasets, performance on the one biomedical dataset they used is among the lowest, having been outperformed by a simple linear probe.

This raises the question of whether domain knowledge can be implicitly plugged into these models, and whether it can enhance their ability to form robust representations of nuanced datasets—particularly those that rely on subtle morphological cues beyond standard visual descriptors. Following this this line of reasoning, we explore whether the need for domain expertise can be addressed through a mixture of these experts, with each building their own bottlenecks and harmonising representations. Specifically, we question whether combining generalist and specialist models can yield concept bottlenecks that are both performant in end-to-end classification and capable of offering fine-grained, semantically grounded interpretability.

A learned gating module adaptively combines individual experts, namely the *generalist* CLIP and the *specialist* BioMedCLIP. Two representative biomedical datasets for dermatoscopy and radiology are chosen to investigate two fundamental research questions:

1. Does domain-specific expertise improve both the interpretability and classification performance across both biomedical domains?

2. Can this mixture-of-experts outperform single-expert baselines, in both fully supervised and few-shot scenarios?

The findings of this work suggest that MoE-based combinations can produce remarkable boosts in performance during full supervision, while building nuanced, independent bottlenecks that select expert-specific features; this is especially profound in the radiology dataset ($\approx 20\% \uparrow$ improvement from the generalist baseline). This work also makes methodological improvements to the LaBO pipeline via more structured prompt engineering and straightforward concept extraction.

While evaluating such architectures in few-shot settings introduces complexity, especially given the limited data available to train a robust gating mechanism, it remains a valuable diagnostic tool to see if a model can leverage prior relationships stored in its bottlenecks to act under constrained supervision. In this setting, the specialist expert consistently outperforms its counterparts, with the MoE having unrepresentative gating policies. Though regularisation techniques encourage more balanced expert usage in few-shot settings, further work is needed to enable stable few-shot deployment, such as by transferring gating priors from adjacent biomedical tasks in ways that do not induce leakage.

2 Related Work

Concept Bottleneck Models (CBMs) improve interpretability by incentivising models to predict human-understandable concepts as an intermediate step before the final prediction [4] In medical imaging tasks like diagnosing arthritis from an X-Ray, a CBM would first predict clinical concepts (e.g. presence of spurs) and then use those concepts to compute severity. Medical practitioners can inspect and intervene on the model's concept predictions. However, traditional CBMs require training labels for each concept and often lag in accuracy compared to their black-ox counterparts. "Label-free" CBMs transform any network into a CBM without per-concept annotations using rudimentary LLMs [5] for concept discovery. Language In a Bottle (LaBO) extended this paradigm with submodular optimisation to filter relevant and discriminative concepts in the same way a human expert would [3].

An orthogonal direction leverages vision-language pre-training to tackle limited labels. CLIP is a foundation model that learns joint image-text representations, and have been proven to transfer to new tasks with little or no task-specific data. In the biomedical domain, variants of the CLIP architecture such as BioMedCLIP were proposed, having been trained on vast amounts of scientific text [6].

The Mixture-of-Experts architecture is a long-standing proposition in deep learning, that dynamically combines the strenghts of multiple specialised models using a divide-and-conquer approach [7, 8]. Recent work has applied MoEs to fuse generalist and specialist knowledge, which is particularly relevant in biomedical imaging where a model, much like a doctor, would require both broad and fine-grained expertise. Med-MoE introduced a mixture-of-experts design for medical VL tasks using multiple domain-specific experts alongside a global meta-expert, replicating how different medical specialties unite to form robust diagnoses; it attained state-of-the-art performance by activating only a few relevant experts instead of the entire model [9]. Furthermore, because gating decisions reveal which experts were consulted and how much importance was given to their analysis, a clinician can trace deeper intuitions. An Interpretable MoE (IME) uses linear models as experts, with each prediction being accompanied by an exact

explanation of which linear expert was used and how it arrived at the outcome [10]. Impressively, this IME approach maintains accuracy comparable to black-box networks, showing that MoE architectures can incorporate interpretability without sacrificing predictive capacity.

A tangentially relevant direction uses a hybrid neuro-symbolic design, routing samples down a tree of interpretable experts to explain a black box [11]. While most prior efforts apply mixture-of-experts to fully supervised, end-to-end deep networks, we explore its extension to concept bottleneck models—specifically probing whether we can align class-concept association matrices rather than purely combining neural embeddings, and whether this remains effective under few-shot constraints.

3 Method

3.1 Biomedical Data

We select (i) HAM10000 (dermatoscopy) and (ii) COVID-QU-Ex (X-Rays) as two representative datasets in the biomedical domain.

HAM10000 is a collection of 10,015 dermatoscopic images representing seven variations of skin lesions[1] that are compiled from various populations [12], and is commonly used as a benchmark dataset for medical vision encoders. We use the same training, validation and testing splits as the dataset providers.

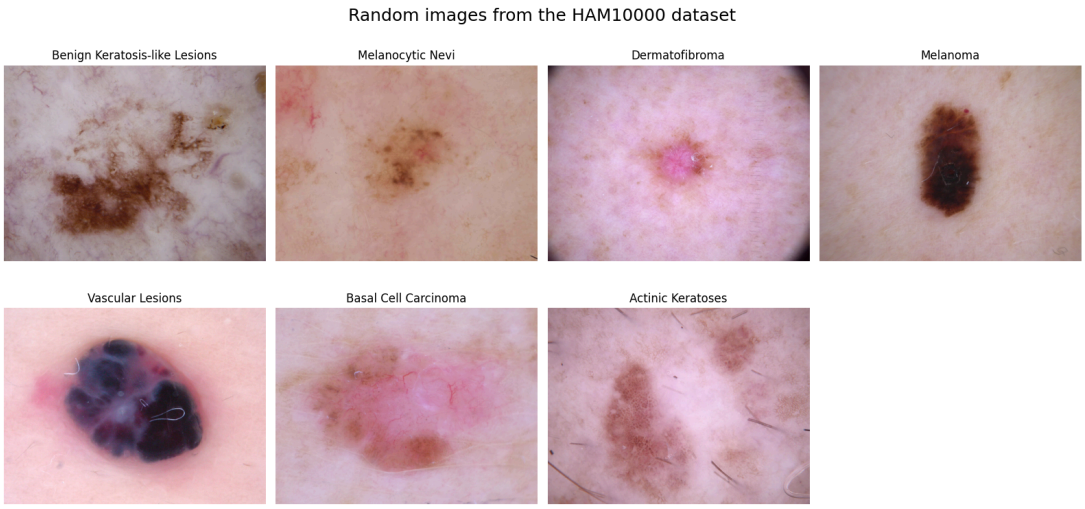

Figure 1: Sample Images from the HAM10000 dataset

The COVID-19 Radiography Database comprises 33,920 posterior–anterior chest X-ray images, covering COVID-19, viral/bacterial pneumonia, and normal cases [13, 14]. It integrates multiple datasets, including COVID-19 cases from Qatar, Italy, Spain, and Bangladesh, alongside pre-pandemic pneumonia datasets from the USA. Training, validation and test splits are While we initially considered the NIH ChestX-ray14 dataset [15], its multi-label nature required sigmoid-activated association matrices within our concept bottleneck setup — leading to gradient explosion during training, making it unsuitable for our architecture.

[1] melanoma, basal cell carcinoma, and benign keratosis-like lesions

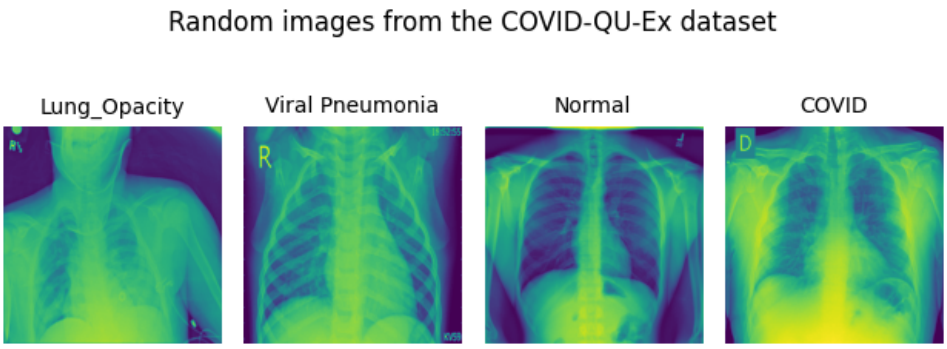

Figure 2: Sample Images from the COVID-QU-Ex dataset

3.2 A Representative Bottleneck

LaBO employed sentence parsing using a T5 to extract semantic concepts from LLM-generated sentences [16]. We conjecture that this approach is suboptimal, leads to information loss and the quality of the final model is dependent on the accuracy of the trained parsing model. Instead, we propose enforcing JSON structure via Pydantic in prompts we send to our LLM suite (LLAMA, DeepSeek, Meditron and OpenAI's 4o), directly extracting phrasal concepts without intermediate parsing [17, 18].

Concepts generated for the generalist are augmented with the phrase: "You can be a bit technical."[2] Our enhanced prompt engineering outperforms the manual parsing algorithm.

Technical Prompt Generation

Background: Extract the concepts from the class to be used for dermatoscopic images. *You can be slightly technical when generating the concepts.*

Prompt: Describe the {*feature*} of the {*disease*} disease in HAM10000 that can be used as visual concepts for Skin Cancer classification.

3.3 Multi-Expert Submodular Optimisation

Submodular optimisation is used to select a discriminative set of concepts that maximise coverage of class semantics while minimizing redundancy. Specifically, we define a set function $f(S) = \alpha \cdot \text{coverage}(S) - \beta \cdot \text{redundancy}(S)$, and select the subset $S \subseteq C$ of concepts by approximately maximizing $f(S)$ via a greedy algorithm. As an improvement to the original paper's algorithm:

1. We incorporate CLIP + BioMedCLIP embeddings into the selection process to account for global similarity. This also implicitly makes sure that only textual concepts that are semantically understood by the VLM are part of the final selection. We modify this architecture for the mixture-of-experts scenario, doing expert-wise bottleneck maintenance.
2. Concepts are stemmed, filtered for stopwords, and pruned to remove any that contain morphological variants of class names — done to reduce semantic leakage and prevent the model from trivially associating concepts with their target classes.

[2] After several rounds of prompt engineering, this produced the best results.

This mechanism proves particularly valuable for advanced biomedical terminology — such as *telangiectasia*, *ovoid* or *keratinization* — which are well-represented in BioMedCLIP's domain corpus but may not be meaningfully encoded by CLIP. By filtering concepts through this embedding-informed scoring process, we obtain a lean and discriminative concept set that adapts to each expert model. As seen in the example concept list, the generalist leans towards visual descriptors, while the specialist uses very specific terminology, whose visual context is implicitly encoded due to the training corpus[3]. It is unsurprising that common words such as "presence", "brown", "areas" and "pigmentation" are widely used in both corpora[4].

Global Specialist Concepts:	**Global Generalist Concepts:**
• Keratinization patterns • Erythematous base • Focal Nodularity • Multilobular pattern ...	• Crusty texture • Small diameter • Pink • Light brown ...

During MoE, we freeze the concept selection bottlenecks, and use those selected during their corresponding uni-expert training cycles. This allows for fair comparisons and ensures that the data distribution is the only independent factor.

3.4 Mixture-of-Experts

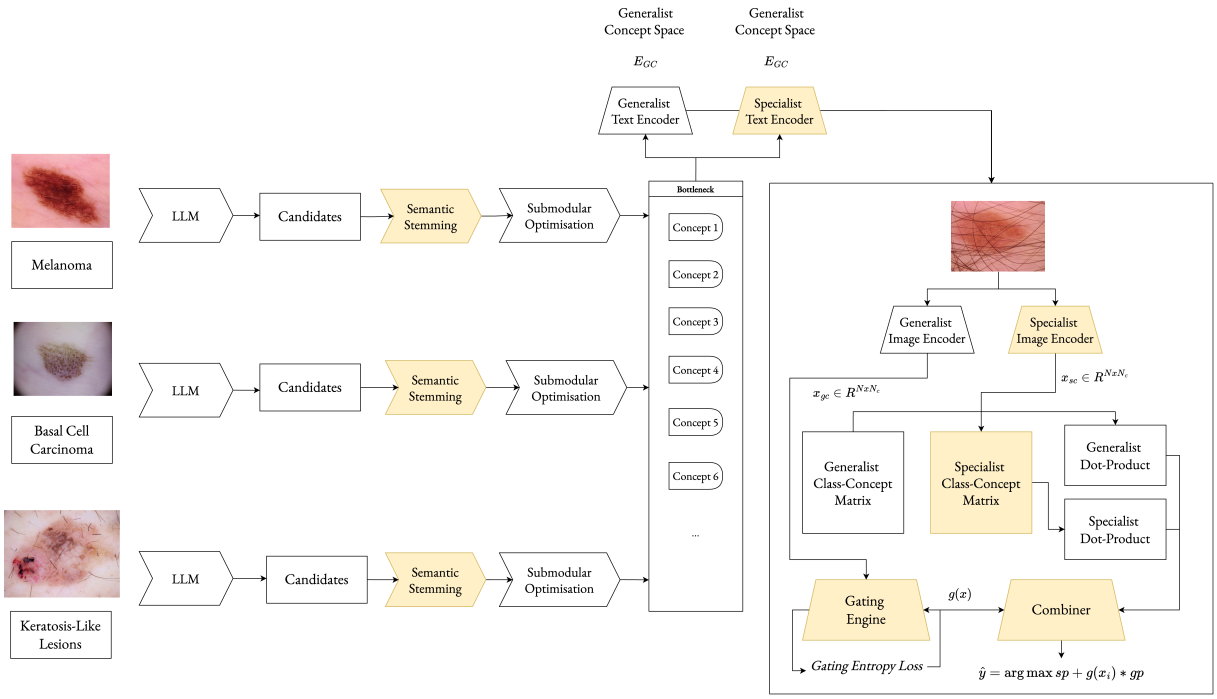

Figure 3: Bottled Brilliance Neural Architecture. Additions to LaBO are highlighted in yellow.

3.4.1 The Case for Expertise

As seen in the selection process, some lesions are distinguishable by general visual attributes like colour patterns and asymmetry, which CLIP catures well [19]. However, we hypothesise that

[3]e.g. "Keratinization is defined as cytoplasmic events that take place"

[4]distributions computed using the nltk toolkits and the CLIP similarity scores

there may be useful biomedical descriptors, that help when attempting to interpret decisions. For instance, a "multilobular pattern" has a distinct morphological shape, that when presented to an ordinary person, would appear obscure, but could highlight a clear analogy to a medical professional who would assess that analogy to build a deeper understanding of the diagnosis. The elucidated scenario comprises of a specialist audience, and a "common man" generalist. When representing this neurally, we find that it is reminiscent of the Mixture-of-Experts architecture [8].

3.4.2 The Experts

CLIP is the choice architecture in LaBO; it learns a transferable visual representation by contrastively training image and text encoders on 400 million (image, text) pairs [19]. It's wide training corpus and general understanding of worldly knowledge makes it a suitable candidate for the generalist. BioMedCLIP is a multimodal biomedical foundation model, trained on PMC-15M, a dataset containing 15 million biomedical image-text pairs that are taken from scientific articles in PubMed Central (PMC). The corpus taxonomy includes dermatology photos, microscopy, histopathology and X-Rays.

To ensure a fair comparison, we standardise the architecture by using ViT-B/16 for both experts, instead of the ViT-L/14 used in LaBO. While ViT-L/14 outperforms the base variant, large-scale BioMedCLIP models are not publicly available; however, scaling laws suggest that performance would improve proportionally by increasing transformer complexity [20].

3.4.3 Formulation

Our Gated Mixture-of-Experts approach combines similarity embeddings from both CLIP (E_C) and BioMedCLIP (E_B). Our approach uses precomputed image-to-concept dot products from each expert, and learns a concept-to-class association matrix for both. Formally, given an input image vector x_i, we pre-compute the generalist and specialist dot products based on their image and concept vectors:

$$\left\{D^g \in \mathbb{R}^{B\times m_g}, D^s \in \mathbb{R}^{B\times m_s}\right\} \tag{1}$$

where m_g and m_s denote the number of generalist and specialist concepts respectively. $A^g \in \mathbb{R}^{K\times m_g}$ and $A^s \in \mathbb{R}^{K\times m_s}$ are learnable association matrices that map concepts to class logits. To encourage semantically meaningful class–concept associations, the individual association matrices are initialised using language model priors by selecting the closest concepts to each class name in the CLIP embedding space.

$$\begin{pmatrix} 1 & 1 & 0 & 0 & 0 & 0 \\ 0 & 0 & 1 & 0 & 1 & 0 \\ 0 & 0 & 0 & 1 & 0 & 1 \end{pmatrix} \tag{2}$$

Weight initialisation for association matrix, where rows = classes, and columns = concepts.

Class-level predictions from each expert are computed as $S^g = D^g \times (A^g)^T$ and $S^s = D^s \times (A^s)^T$.

The gating network, tuned to inhibit over-parametrisation, is a two-layer neural network with a *LeakyReLU* activation and sigmoid output, defined as:

$$g(x_i) = \sigma(W_2(\text{LeakyReLU}(W_1(\text{LayerNorm}(x_i))))) \tag{3}$$

$g(x_i) \in [0, 1]$ dynamically determines the cross-expert weighting for each input and produces a weighted combination:

$$S_i = g(x_i) \cdot S_i^s + (1 - g(x_i)) \cdot S_i^g \tag{4}$$

The Gated MoE model is trained by minimizing a total loss that consists of a classification loss (cross-entropy for single-label and binary cross-entropy for multi-label) and a gate entropy loss, that encourages the gating network to avoid overly deterministic decisions and completely depend on one of the experts (by collapsing $g(x_i) \to \{0, 1\}$). Additional regularisers are added to encourage prediction diversity (disincentivize model from collapsing similarity scores) and sparse concept-to-class activations[5]. In the results section, we share an ablation between different loss combinations.

$$\mathcal{L} = \text{CrossEntropy}(S, y) + \lambda_{\{\div\}} \cdot \left(-E_{\{i\}}\left[\text{Var}_{\{k\}}\left(S_{\{i,k\}}\right)\right]\right) + \lambda_{\{\text{L1}\}} \cdot (\|A^g\|_1 + \|A^s\|_1) \tag{5}$$

3.5 Experimental Infrastructure

All experiments were run on a single NVIDIA L40S GPU in the Department of Computer Science's GPU server, while Weights and Biases is used for experimental tracking [21]. We run all few-shot models for a maximum of 5000 epochs and run tests based on the best validation performance[6]. To tackle the cold start issue for noisy gate parameters under few-shot scenarios, a 500 epoch warm start is allowed, where the only trainable parameters are the gate.

When running the experiments for the first time, a bug in the mixture of experts code that combined 2

4 Results

4.1 Loss Ablation

Primary hyperparameter tuning is done on HAM10000, with the best configurations immediately ported over to COVID-QU-Ex.

Variation	**Validation Accuracy**					
	1-shot	2-shot	4-shot	8-shot	16-shot	All
MoE	0.314	0.464	0.248	**0.439**	0.464	**0.792**
$\text{MoE}_{\text{entropy}}$ ($\lambda = 0.2$)	**0.482**	**0.494**	0.248	0.346	**0.539**	0.786

Table 1: Shot-by-Shot Results

The use of our gating entropy loss provides performance boosts in three of five shots (with an average improvement of 6.19%), representative of its utility in stabilising gate estimates, with an average and discouraging the gating network from collapsing too early to a single expert. The weighting λ_{entropy} for the entropy loss component is set at 0.2, to avoid saturating the loss computation.

4.2 Fully Supervised Baselines

We first evaluate the models in the complete models in a fully supervised setting. The original paper uses `ViT-L/14` in their architecture. However, for the sake of fair comparisons, we

[5]the original paper did not employ these losses in their final ablations, so we replicate those same decisions

[6]tuned to prevent overfitting where the training accuracy can quickly hit 100% due to under-parametrisation

Model Variant	Val. Acc. (%)	Val. Loss	Test Acc. (%)	Test Loss
ViT-B/16	79.1	0.5501	76.8	0.6126
BioMedCLIP	77.3	0.69656	75.03	0.7916
MoE	**79.6**	4.442	**78.61**	0.714

Table 2: Individual Model Performance Results

Under fully supervised conditions, standard CLIP still outperforms BioMedCLIP, likely because ample supervision allows for a sufficiently comprehensive representation—lessening the advantage of specialized domain expertise. The best performance is attained by the Mixture of Experts (MoE), outperforming both uni-expert counterparts by $\approx 4.66\%$. However, the elevated loss suggests that, while the model achieves strong accuracy, its occasional errors are highly confident misclassifications — potentially exacerbated by the gating mechanism's sharp routing decisions. When analysing the average gate distribution, we find that the gate's $g(x_i)$ begins to fluctuate before reaching a batch-wise average of 0.8 by the final training epoch. This shows increased dependence on the specialist in the majority of cases.

4.3 Skin Lesion Classification

Architecture	Validation Accuracy					Test Accuracy				
	1-shot	2-shot	4-shot	8-shot	16-shot	1-shot	2-shot	4-shot	8-shot	16-shot
G (PC)	23.0	35.9	24.4	34.5	53.0	22.4	38.1	23.4	31.9	52.6
S	25.0	38.8	**49.4**	**63.0**	52.8	27.2	40.0	**48.8**	**61.7**	52.3
MoE	31.4	46.4	24.8	43.9	46.4	28.1	48.1	27.3	42.9	45.1
$\text{MoE}_{\text{entropy}}$	**48.2**	**49.4**	24.8	34.6	**54.6**	**45.8**	**50.2**	23.5	34.2	**52.8**

Table 3: Shot-by-Shot Results (in %) -

The specialist expert outperforms its counterparts by a substantial margin in ultra-low-shot settings (1-2 shots), showing that domain-specific knowledge provides strong performance boosts when there is minimal labelled data. However, under high-supervision and full-supervision, the specialist advantage diminishes, with the generalist outperforming it as soon as there is enough data to learn broad visual features and enrich the association matrix.

Interestingly, the Mixture-of-Experts excels at ultra-low-shot scenarios, where MoE partial insights are fused from both experts to provide surprisingly impressive performance ($> 70\%$) improvement. It must however be noted that the weights learned by gate may be suboptimal when there isn't sufficient supervision to enrich weighting decisions; in early epochs, the average gate weight $g(x_i)$ edges wavers $0.4 \leftrightarrow 0.6$ Under mid-range supervision, the results do not consistently favour MoE, since partial supervision is likely insufficient for the gate to converge on an optimal blend, adversely hurting performance instead.

A general observation is that the mixture-of-experts lacks sufficient supervision in few-shot settings to train a sufficiently rich gate, with the full benefits of combining experts only visible during full supervision. There is also near-random and unexplainable fluctuations in 4- and 8- shots.

4.3.1 Intuition about Foundation Gates

One solution to this problem would be to train the gate on a tangentially similar task and port the weights, so the starting representation would have some intuition about which types of images would be suitable for which expert. However, this would require clear cross-task alignment, and there is little formal proof to support this conjecture.

4.4 Gating Fluctuations

The gate provides fascinating insights into the inner workings of the model. Across 1- to 2-shot settings, there is a dramatic fluctuation in $g(x)$ as it lacks sufficient training examples to learn a stable preference, bouncing back between near-0 and near-1. In the mid-shot graphs (4-shot and 8-shot), the gate still oscillates in phases but displays a modestly smoother pattern – though there are steep dips towards 0 or 1 at certain epochs; likely indicative of preference collapses. By 16-shot, the trend stabilises, with a surprising number of samples favouring the generalist over the specialist. Under fully supervised training, the network has enough labels to make more confident routing decisions, with the histogram staying relatively consistent across epochs. Unsurprisingly, the specialist is favoured when all training samples are considered. Overall, it seems clear that sufficient supervision is necessary for the gate to build a stable representation.

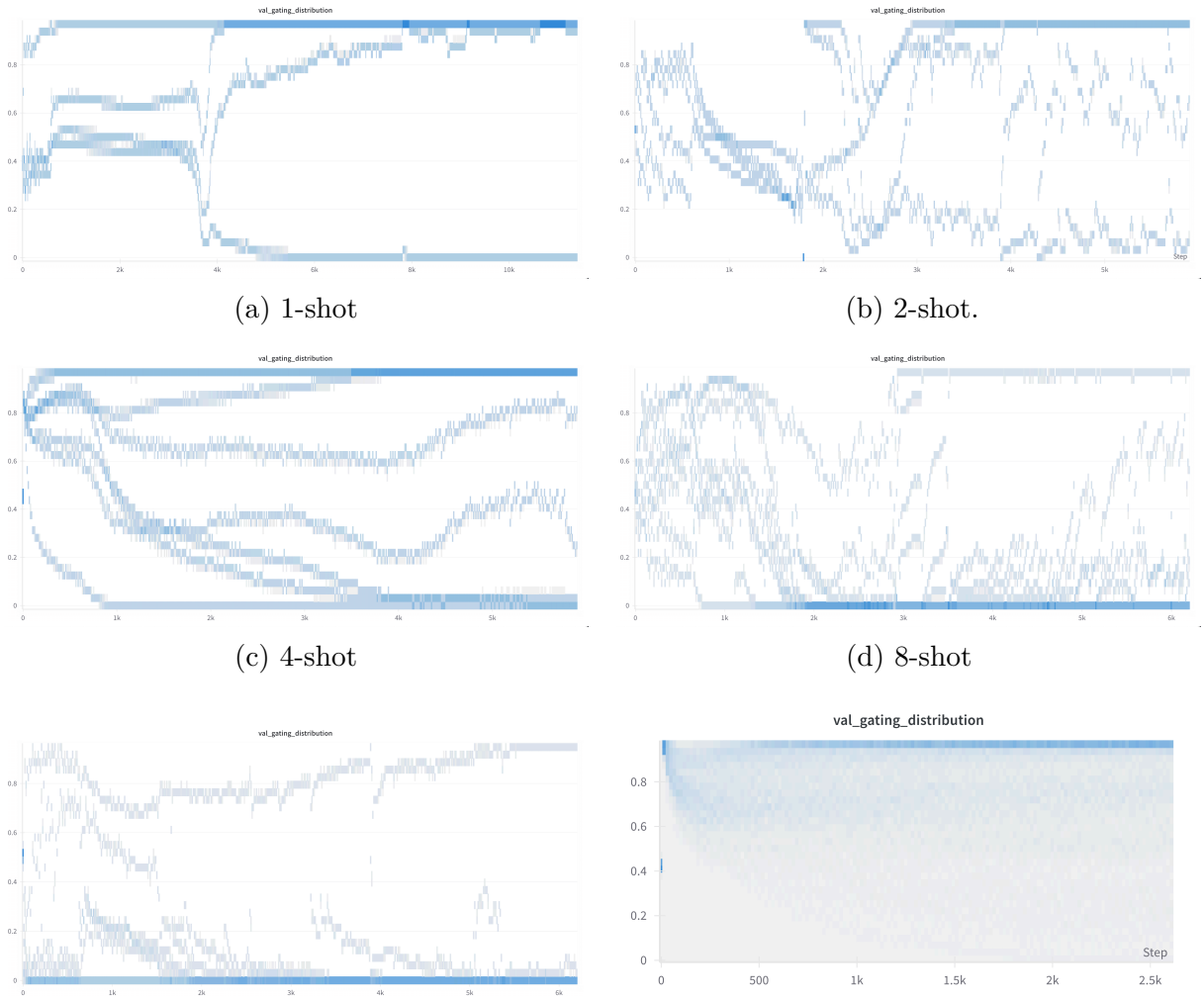

(a) 1-shot (b) 2-shot.

(c) 4-shot (d) 8-shot

(e) 16-shot (f) All-shot

Figure 4: Gating Distribution Acros Different Shots

4.5 COVID-QU-Ex

Arch.	Validation Accuracy						Test Accuracy					
	1-shot	2-shot	4-shot	8-shot	16-shot	All	1-shot	2-shot	4-shot	8-shot	16-shot	All
G	44.4	48.09	46.94	59.20	64.93	87.36	43.96	47.86	45.81	58.94	63.57	86.6
S	39.0	40.48	**69.65**	**68.79**	67.7	89.93	38.53	41.06	**69.41**	**68.04**	69.22	89.89
MoE	**45.62**	**65.87**	51.76	61.88	**78.62**	**93.51**	**47.20**	**63.69**	50.06	61.90	**77.61**	**93.67**

Table 4: Shot-by-Shot Results (in %) for COVID-QU-Ex

In extreme low-shot cases (1-2 shots), MoE significantly outperforms both the generalist and the specialist, suggesting that fusing domain-specific cues help overcome the data scarcity. Furthermore, we observe in the gating histogram that there is an even balance between the generalist and specialist weights ($0.2 < g(x) < 0.6$), suggesting that both experts are equally consulted in low-shot scenarios. However, at 4-8 shots, the specialist begins to outperform it's counterparts, eclipsing gains from the gated combination of both experts. By 16-shots, there is sufficient supervision for the gating network to converge on a better routing algorithm for each individual sample, with MoE taking the lead and outperforming the specialist by $\approx 11\%$.

Under full supervision, MoE attains the highest accuracy of all, with an outstanding accuracy of 93.67%, consistent with the hypothesis that enough labelled data can produce remarkable synergies. The gating distribution histogram in Figure 5 shows a sparse distribution of gate values, with a significant number prioritising the specialist towards the end of training, reflecting the value of domain-specific representations for X-Ray data.

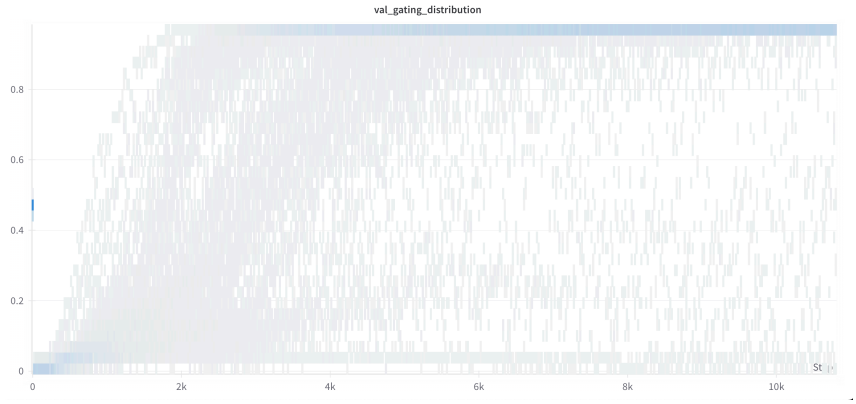

Figure 5: Fully Supervised Gating Distribution for Covid-X

The specialist is also consistently strong across all shots, with incremental improvements as more data is appended – unlike in dermatoscopy where the generalist eventually catches up other full supervision. BioMedCLIP was trained with an extensive volume of X-Ray data (10^6 samples), an order of magnitude higher than dermatoscopic samples. Crucially, X-Ray classification often hinges on subtle clinical markers (e.g. faint opacities, lesions) which are difficult to identify on a purely visual or textural level, requiring domain-specific context and known prior connections in the scientific literature to help the model make accurate diagnoses.

5 Conclusion and Limitations

In this work, we introduce a Mixture-of-Experts extension to concept bottleneck models, designed to fuse domain-specific knowledge with a more general visual understanding. The architecture learns a gate between experts to make weighting decisions, and is particularly remarkable under full-supervision, where there is sufficient training data to learn a strong gate representation. The hypotheses are validated across HAM10000 (dermatoscopy) and COVID-QU-Ex (chest X-rays).

However, few-shot performance is still relatively unstable, despite regularisation methods, and it is notably difficult to sufficiently understand a dataset to efficiently synergise the experts. Future work can pre-train the gating network on related biomedical tasks (X-Ray Gate $\leftrightarrow$ Dermatoscopy Gate), initialising it in our MoE framework with a general intuition for expert selection. Furthermore, due to computational constraints, the individual experts have their encoders frozen in the current architecture. An intriguing next step would be to allow partial fine-tuning or cross-expert transfer learning through residual connections [22], potentially further aligning the experts' representations while preserving their distinct domain-specific strengths.

6 Notes

- Using ViT-B/16 to establish the baseline in this paper - because it outputs 512 dimensions, which is the same as MedCLIP and BioMedCLIP
- Motivation - biomedical explainability is important - do more specialised variants do a better job
- We can't directly assess the quality of the explanation, but we can implicitly assess them through the expressiveness of the concept alignment
- Hypothesis - combine generalist + specialist improve interpretability and concepts
- Try initialising association weights using `gen_init_weight_from_cls_name` – might be useful in few-shot scenario
- Some of the accuracies in the table were from the last epoch, not the best epoch - make sure to check

6.1 Research Questions

1. First, does separating concept spaces improve interpretability and classification performance?
2. Second, can learned fusion weights outperform naive averaging of similarity scores?
3. And third, does the specialist model contribute more on rare or complex conditions?

6.2 Methodology

- Run individual models - done
- Run BioMedCLIP with more specialised features
- Do hybrid gating between MedCLIP and BioMedCLIP - use different concept sets - only modify asso_opt.py file
- CLIP explainability - https://colab.research.google.com/github/hila-chefer/Transformer-MM-Explainability/blob/main/CLIP_explainability.ipynb#scrollTo=3ogYpvQAAH4s

If there's time:

- Linear probe NIH-XRay
- Apply best method from above

7

Bibliography

[1] H. Xu and K. M. J. Shuttleworth, "Medical artificial intelligence and the black box problem: a view based on the ethical principle of "do no harm," *Intelligent Medicine*, vol. 4, no. 1, pp. 52–57, 2024, doi: https://doi.org/10.1016/j.imed.2023.08.001.

[2] C. Rudin, "Stop explaining black box machine learning models for high stakes decisions and use interpretable models instead," *Nature Machine Intelligence*, vol. 1, no. 5, pp. 206–215, May 2019, doi: 10.1038/s42256-019-0048-x.

[3] Y. Yang, A. Panagopoulou, S. Zhou, D. Jin, C. Callison-Burch, and M. Yatskar, "Language in a bottle: Language model guided concept bottlenecks for interpretable image classification," in *Proceedings of the IEEE/CVF Conference on Computer Vision and Pattern Recognition*, 2023, pp. 19187–19197.

[4] P. W. Koh *et al.*, "Concept Bottleneck Models," in *Proceedings of the 37th International Conference on Machine Learning*, H. D. III and A. Singh, Eds., in Proceedings of Machine Learning Research, vol. 119. PMLR, 2020, pp. 5338–5348. [Online]. Available: https://proceedings.mlr.press/v119/koh20a.html

[5] T. Oikarinen, S. Das, L. M. Nguyen, and T.-W. Weng, "Label-free Concept Bottleneck Models," in *International Conference on Learning Representations*, 2023.

[6] S. Zhang *et al.*, "A Multimodal Biomedical Foundation Model Trained from Fifteen Million Image–Text Pairs," *NEJM AI*, vol. 2, no. 1, p. AIoa2400640, 2025, doi: 10.1056/AIoa2400640.

[7] X. Yang *et al.*, "Mixture of Experts Made Intrinsically Interpretable." [Online]. Available: https://arxiv.org/abs/2503.07639

[8] D. Eigen, M. Ranzato, and I. Sutskever, "Learning Factored Representations in a Deep Mixture of Experts." [Online]. Available: https://arxiv.org/abs/1312.4314

[9] S. Jiang, T. Zheng, Y. Zhang, Y. Jin, L. Yuan, and Z. Liu, "Med-MoE: Mixture of Domain-Specific Experts for Lightweight Medical Vision-Language Models," in *Findings of the Association for Computational Linguistics: EMNLP 2024*, Y. Al-Onaizan, M. Bansal, and Y.-N. Chen, Eds., Miami, Florida, USA: Association for Computational Linguistics, Nov. 2024, pp. 3843–3860. doi: 10.18653/v1/2024.findings-emnlp.221.

[10] A. A. Ismail, S. Ö. Arik, J. Yoon, A. Taly, S. Feizi, and T. Pfister, "Interpretable Mixture of Experts for Structured Data," *ArXiv*, 2022, [Online]. Available: https://api.semanticscholar.org/CorpusID:249394928

[11] S. Ghosh, K. Yu, F. Arabshahi, and K. Batmanghelich, "Dividing and Conquering a BlackBox to a Mixture of Interpretable Models: Route, Interpret, Repeat," in *Proceedings of the 40th International Conference on Machine Learning*, A. Krause, E. Brunskill, K. Cho, B. Engelhardt, S. Sabato, and J. Scarlett, Eds., in Proceedings of Machine

Learning Research, vol. 202. PMLR, 2023, pp. 11360–11397. [Online]. Available: https://proceedings.mlr.press/v202/ghosh23c.html

[12] P. Tschandl, C. Rosendahl, and H. Kittler, "The HAM10000 dataset, a large collection of multi-source dermatoscopic images of common pigmented skin lesions," *Scientific Data*, vol. 5, no. 1, Aug. 2018, doi: 10.1038/sdata.2018.161.

[13] T. Rahman *et al.*, "Exploring the effect of image enhancement techniques on COVID-19 detection using chest X-ray images," *Computers in Biology and Medicine*, vol. 132, p. 104319, 2021, doi: https://doi.org/10.1016/j.compbiomed.2021.104319.

[14] M. E. H. Chowdhury *et al.*, "Can AI Help in Screening Viral and COVID-19 Pneumonia?," *IEEE Access*, vol. 8, no. , pp. 132665–132676, 2020, doi: 10.1109/ACCESS.2020.3010287.

[15] X. Wang, Y. Peng, L. Lu, Z. Lu, M. Bagheri, and R. M. Summers, "ChestX-ray8: Hospital-scale Chest X-ray Database and Benchmarks on Weakly-Supervised Classification and Localization of Common Thorax Diseases," *CoRR*, 2017, [Online]. Available: http://arxiv.org/abs/1705.02315

[16] C. Raffel *et al.*, "Exploring the Limits of Transfer Learning with a Unified Text-to-Text Transformer," *CoRR*, 2019, [Online]. Available: http://arxiv.org/abs/1910.10683

[17] H. Touvron *et al.*, "LLaMA: Open and Efficient Foundation Language Models." [Online]. Available: https://arxiv.org/abs/2302.13971

[18] DeepSeek-AI *et al.*, "DeepSeek-R1: Incentivizing Reasoning Capability in LLMs via Reinforcement Learning." [Online]. Available: https://arxiv.org/abs/2501.12948

[19] A. Radford *et al.*, "Learning Transferable Visual Models From Natural Language Supervision," in *Proceedings of the 38th International Conference on Machine Learning, ICML 2021, 18-24 July 2021, Virtual Event*, M. Meila and T. Zhang, Eds., in Proceedings of Machine Learning Research, vol. 139. PMLR, 2021, pp. 8748–8763. [Online]. Available: http://proceedings.mlr.press/v139/radford21a.html

[20] X. Zhai, A. Kolesnikov, N. Houlsby, and L. Beyer, "Scaling Vision Transformers," in *Proceedings of the IEEE/CVF Conference on Computer Vision and Pattern Recognition (CVPR)*, Jun. 2022, pp. 12104–12113.

[21] L. Biewald, "Experiment Tracking with Weights and Biases." [Online]. Available: https://www.wandb.com/

[22] H. Zhao, Z. Qiu, H. Wu, Z. Wang, Z. He, and J. Fu, "HyperMoE: Towards Better Mixture of Experts via Transferring Among Experts." [Online]. Available: https://arxiv.org/abs/2402.12656

APPENDIX A

A.1 Prompt Generation

A.2 Ablation Study on Mixture-of-Experts

Arch.	**Validation Accuracy**						**Test Accuracy**					
	1	2	4	8t	16	All	1	2	4	8	16	All
G (PC)	0.230	0.359	0.244	0.345	**0.546**	—	0.2239	0.3811	0.2338	0.3194	**0.5284**	—
G (OC)	0.335	0.312	0.308	0.323	0.530	0.810	0.3095	0.3443	0.2915	0.3114	0.540	0.769
S	0.250	0.388	**0.494**	**0.630**	0.528	—	0.2716	**0.40**	**0.488**	**0.617**	0.5234	0.7503
MoE (st.)	0.314	0.464	0.248	0.439	0.464	0.792	0.2806	0.4806	0.2726	0.4289	0.4508	**0.772**
MoE (st.)	**0.482**	**0.494**	0.248	0.346	0.539	0.786	**0.458**	**0.502**	0.2348	0.3423	0.5114	0.7592

Table 5: Shot-by-Shot Results